

Assessing the Impact of Precipitation Change on Design Annual Runoff in the Headwater Region of Yellow River, China

Y. M. Hu^{1,2}, Z. M. Liang^{1*}, D. P. Solomatine^{3,4}, H. M. Wang², and T. Liu¹

¹College of Hydrology and Water Resources, Hohai University, Nanjing 210098, China

²Research Institute of Management Science, Business School, Hohai University, Nanjing 211100, China

³UNESCO-IHE Institute for Water Education, Delft 2601 DA, Netherlands

⁴Water Resources Section, Delft University of Technology, Delft 2600 AA, Netherlands

Received 13 April 2017; revised 04 April 2018; accepted 09 October 2018; published online 17 October, 2019

ABSTRACT. A significant decrease in annual runoff (AR) in the headwater region of Yellow River, China, has been observed during the past decades, which produces a recognized impact on long-term water resources management and planning. In this paper, the Pettitt method and Sequential Clustering method are used to detect the change point of AR and annual precipitation (AP) series. On the basis of the change point, the whole observed period is divided into two periods, before-point (Period I) and after-point period (Period II). The distribution characteristic of occurrence number of given extreme AP and AR and the relationship between the AP and AR in the two periods are analyzed. Then, the impact of AP change on the design AR is quantified. The results indicate that the AP and AR has a change point at the location of 1989. The distribution of occurrence number of given AP with more than 500 mm and AR with more than 150 mm in Period I is clearly different than that in Period II as well as the AP-AR relationship. The quantiles of AP and AR with the given non-exceedance probabilities of 0.8, 0.9, 0.95, 0.98, 0.99, 0.995, 0.998 and 0.999 in Period I decrease significantly compared to those in Period II. The AP decrease accounts for 53, 53, 54, 57, 60, 62, 66 and 68% of the total decrease in AR at the level of quantile with respect to the given eight non-exceedance probabilities from 0.8 to 0.999. Overall, the decrease in the AR quantile is mainly caused by the decrease in AP change.

Keywords: water resource, annual runoff; precipitation change

1. Introduction

Over the past several decades, climate change and human activities have produced significant impacts on water resources in some parts of the world, featuring a decreasing or increasing trend, which has been reported in many literature and received great attention from researches, decision makers and the general public (Boyer, 2010; Guo, 2013; Ye, 2013; Pina et al., 2016).

In order to better understand the impact of climate change and human activities on water resources, a large number of studies have been carried out. Legesse et al. (2003) utilized a distributed precipitation-runoff model to study hydrological response of a catchment to climate and land use changes in tropical Africa. Their analysis indicated that a 10% decrease in rainfall and 1.5 °C increase in air temperature produced a 30 and 15% reduction on the simulated discharge respectively. Ma et al. (2010) employed a hydrological model and a climate elasticity model to estimate the impact of climate change and human activity on runoff decrease in the Miyun Reservoir catchment in China. Their results showed that climate impact was ac-

countable for about 55 to 51% of the decrease in reservoir inflow, while 18% was caused by indirect impact of human activity. Shi et al. (2007) and Miller et al. (2014) investigated the urbanization impact on surface runoff and storm runoff. They demonstrated that urbanization led to obvious increase in the peak flows and decrease in runoff confluence time. Bao et al. (2012) used the Variable Infiltration Capacity (VIC) model to investigate climate change and human activities impacts on various catchments in Haihe basin, China. The results showed that the decrease of runoff could be attributed to climate variability (human activities) by 58.5(41.5), 40.1(59.9) and 26.1% (73.9%) in Taolinkou, Zhangjiafen and Guantai catchments, respectively. Öztürk et al. (2013) developed a land use dynamic model coupled with a spatially distributed three-dimensional surface-subsurface hydrologic model to assess the impact of land use change on the watershed hydrological processes. Wang et al. (2016) analyzed the 15-day, 30-day, and 60-day extreme rainfall change in the next 50 years in the upper basin of the Yellow River basin based on dynamical climate model product (BCC-CSM-1.1), which was used as input for a SWAT model of design rainfall to assess the impact of climate change on corresponding design floods.

Yellow River, also called the “Mother River”, is the second largest river in China. During the past decades, its basin and meteorological conditions have undergone considerable

* Corresponding author. Tel.: +86 10 83786475; fax: +86 10 83786475.
E-mail address: zmliang@hhu.edu.cn (Z. M. Liang).

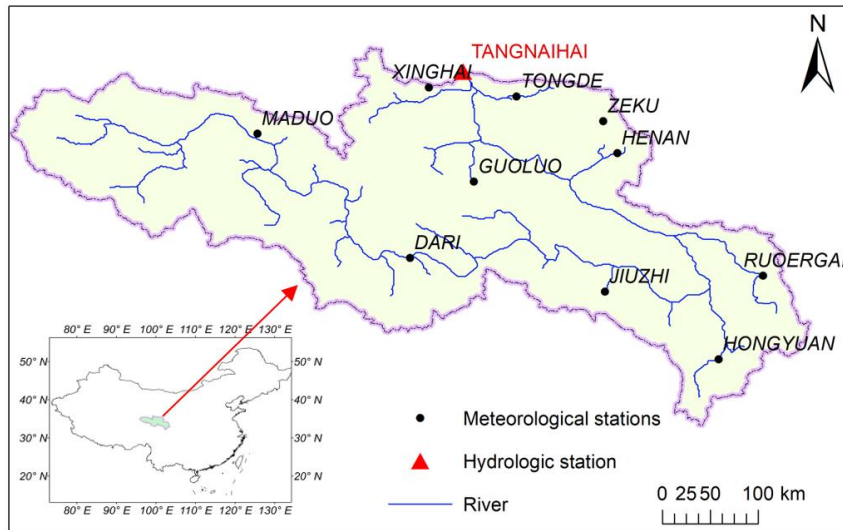


Figure 1. Distribution of hydrological and meteorological stations in Tangnaihai Basin.

changes (Yang et al., 2004; Xie, et al., 2006; Huang et al, 2009). For example, Yang et al. (2004) and Huang et al. (2009) reported that the trends in precipitation haven been constantly negative while temperature was increasing during the last half century. Li et al. (2007) assessed the impact of climate change and human activity on river runoff in the Wudinghe River in China. The results showed that the soil conservation measures account for 87% of the total reduction in annual mean runoff in the period from 1972 to 1997, and the reduction of annual mean runoff due to changes in precipitation and potential evaporation was 13%. Guo et al. (2013) investigated the impact of climate change and land cover/use transition on the hydrology in the upper Yellow River basin. They found that the runoff decrease in the area above Tangnaihai was primarily influenced by climate change.

To our knowledge there has been no study in the headwater region of Yellow River to analyze the impact of annual precipitation (AP) change on design annual runoff (AR) at the level of quantile with respect to a given probability. To have this assessment is very important for decision makers to develop the long-term measures and policy for water resources management and planning as design annual runoff is a commonly used and important index to assess the richness degree of water resources. In this paper, we firstly test the AP and AR series and then propose a method to quantitatively assess the contribution of AP change to the AR at the level of quantile in the headwater region of Yellow River (above Tangnaihai Station). In comparison to the use of a hydrological model to simulate the climate change impact, the proposed method needs less data, which makes it relatively easier to implement.

2. Materials and Methods

2.1. Study Area and Data

The area above the Tangnaihai (TNH) Hydrometric Station is generally regarded as the headwater region of Yellow River, which is located between 95 ° ~ 103 °E longitude and 32 °

~ 35 °N latitude. Its catchment area accounts for about 16% of the whole Yellow River basin area of 752,000 km². The AP ranges from 250 to 750 mm and the average AP is about 487 mm for the period 1958 ~ 2007. Eighty percent of the AP occurs during May-September. The average AR is about 20.47 billion m³, which constitutes about 35% of the average AR of the whole Yellow River basin. The data of AP and AR used here is from 1958 to 2007. The AP of the catchment is calculated by using the Thiessen polygon approach to weight-average the AP of 10 meteorological stations (Figure 1) and the AR is measured at the TNH Hydrometric Station (Figure 1).

2.2. Change Point Detection Method

The Pettitt method (Pettitt, 1979) and the Sequential Clustering method (Ding et al., 1986) are used to detect the location of change point of AP and AR series. On the basis of the change point, the whole series of AP and AR are divided into the two-subseries, i.e., before-point series and after-point series respectively.

For a given series x_1, x_2, \dots, x_n , the test statistic of Pettitt method used to verify if the series is generated from the same population distribution can be calculated in accordance to Pettitt (1979):

$$U_{t,n} = U_{t-1,n} + V_{t,n}, t = 2, 3, \dots, n \quad (1)$$

$$V_{t,n} = \sum_{j=1}^n \text{sign}(x_j - x_t) \quad (2)$$

$$\text{sign}(x_j - x_t) = \begin{cases} +1, & x_j - x_t > 0 \\ 0, & x_j - x_t = 0 \\ -1, & x_j - x_t < 0 \end{cases} \quad (3)$$

By maximizing Equation (1), the change point τ can be

obtained:

$$K_\tau = \max_{1 \leq t \leq n} \{ |U_{t,n}| \} \quad (4)$$

The associated probability PoA of the change point τ is computed in accordance to Pettitt (1979):

$$PoA \equiv 2\exp\{-6(K_\tau)^2/(n^2 + n^3)\} \quad (5)$$

where if $PoA < 0.05$, it means there is a significant change point at the location of τ .

The Sequential Clustering (SC) method can be described in accordance to Ding (1986):

$$W_\tau = \sum_{i=1}^t (x_i - \bar{x}_\tau) \quad (6)$$

$$W_{n-\tau} = \sum_{j=\tau+1}^n (x_j - \bar{x}_{n-\tau}) \quad (7)$$

where \bar{x}_τ and $\bar{x}_{n-\tau}$ are the average values of the series x_1, x_2, \dots, x_τ and $x_{\tau+1}, \dots, x_n$, respectively.

The change point τ can be obtained by minimizing the sum of W_τ and $W_{n-\tau}$:

$$\tau = \min \{ W_\tau + W_{n-\tau} \}, t = 2, 3, \dots, n \quad (8)$$

2.3. Quantile Estimation of AP and AR

On the basis of the observed AP and AR series, the quantiles of AP and AR with given non-exceedance probabilities can be estimated by means of hydrological frequency analysis method (CWRC, 1995; ASCE, 1996). In this study, the Pearson Type Three distribution (PE3) is adopted to estimate the quantiles of AP and AR with the consideration that the PE3 is widely used and recommended in China (CWRC, 1995). Let X denotes the AP or AR, the PE3 probability distribution function is defined (Liang et al., 2014):

$$f(x) = \frac{\beta^\alpha}{\Gamma(\alpha)} (x - a_0)^{\alpha-1} e^{-\beta(x-a_0)} \quad (9)$$

where x is a realization of X with $x \geq a_0$; a_0 , β , and α are the location, scale and skewness parameter of the PE3 function respectively; and $\Gamma(\cdot)$ denotes the gamma function. In addition, the following identical equations for the PE3 distribution are available:

$$a_0 = E(X) - \frac{2\sigma}{C_s}, \beta = \frac{2}{\sigma C_s}, \alpha = \frac{4}{C_s} \quad (10)$$

where $E(\cdot)$, σ , and C_s represent the expectation, standard deviation, and coefficient of skewness of PE3 distribution respectively.

The parameters $E(\cdot)$, σ and C_s can be calculated in accordance to Hosking and Wallis (1997):

$$E(x) = \lambda_1 \\ \sigma = \lambda_2 \pi^{1/2} t^{1/2} \Gamma(t)/\Gamma(t+1/2), C_s = 2t^{-1/2} \text{sign}(\tau_3) \quad (11)$$

where $\tau_3 = \lambda_3/\lambda_2$ and t is computed by the following equations:

If $0 < \text{abs}(\tau_3) < 1/3$, let $z = 3\pi\tau_3^2$, then:

$$t = \frac{1 + 0.2906z}{z + 0.1882z^2 + 0.0442z^3} \quad (12)$$

If $1/3 < |\tau_3| < 1$, let $z = 1 - |\tau_3|$, then:

$$t = \frac{0.36067z - 0.59567z^2 + 0.25361z^3}{1 - 2.78861z + 2.56096z^2 - 0.77045z^3} \quad (13)$$

In Equation (11), the parameters λ_1 , λ_2 , and λ_3 can be obtained:

$$\begin{aligned} \lambda_1 &= \beta_0 \\ \lambda_2 &= 2\beta_1 - \beta_0 \\ \lambda_3 &= 6\beta_2 - 6\beta_1 + \beta_0 \end{aligned} \quad (14)$$

where β_r , $r = 1, 2, 3$ are the probability weighted moments (Greenwood et al., 1979). For a sample series in ascending order, an unbiased sample estimator of β_r (denoted as b_r) can be computed by the following equations:

$$\begin{aligned} b_0 &= \frac{1}{n} \sum_{i=1}^n x_i \\ b_1 &= \frac{1}{n} \sum_{i=2}^n \frac{i-1}{n-1} x_i \\ b_2 &= \frac{1}{n} \sum_{i=3}^n \frac{(i-1)(i-2)}{(n-1)(n-2)} x_i \end{aligned} \quad (15)$$

Then, the parameters of location a_0 , scale β , and skewness α of the PE3 distribution are calculated by Equation (10).

2.4. Quantification of AP Change Impact on AR

Let $X = \{x_1, x_2, \dots, x_n\}$ and $Y = \{y_1, y_2, \dots, y_n\}$ represents the AP and AR series respectively. Based on the change point τ of AP and AR series, the whole period is divided into two different periods: the before-point period (Period I) and the after-point period (Period II). In Period I, the AP and AR series are $(X^I, Y^I) = \{(x_1, y_1), (x_2, y_2), \dots, (x_\tau, y_\tau)\}$ and in Period II, the AP and AR series are $(X^{II}, Y^{II}) = \{(x_{\tau+1}, y_{\tau+1}), (x_{\tau+2}, y_{\tau+2}), \dots, (x_n, y_n)\}$.

With the purpose of quantifying the impact of AP change on AR at the level of quantile with given non-exceedance probabilities from Period I to Period II, the following procedures are designed:

Step 1: Capture the dependence structure between the AP quantile and AR quantile in Period I.

On the basis of the series of AP and AR in Period I, the quantiles of AP (AP_q^I) and AR (AR_q^I) with the given non-exceedance probabilities of 0.8, 0.9, 0.95, 0.98, 0.99, 0.995, 0.998 and 0.999 are estimated respectively by using the hydrological frequency analysis method (Section 2.3). Then the dependence structure between the AP quantile and AR quantile in Period I can be defined by the following statistical model:

$$AP_q^I = f_I(AR_q^I) \quad (16)$$

where AP_q^I and AR_q^I denote the quantiles of AP and AR in Period I; $f_I(\cdot)$ is a function needed to be determined.

Similarly, based on the series of AP and AR in Period I, the dependence structure between the quantiles of AP and AR in Period II can be also obtained:

$$AP_q^{II} = f_{II}(AR_q^{II}) \quad (17)$$

where AP_q^{II} and AR_q^{II} denote the quantile of AP and AR in Period II; $f_{II}(\cdot)$ is a function needed to be determined.

It is certain that if there is no impact of climate change and human activities on the AP and AR, the dependence structure between the quantiles of AP and AR should be uniform in the two different periods.

Step 2: Quantify the impact of AP change on AR at the level of quantile from Period I to Period II.

The total change ΔAR_q of AR quantile with a given non-exceedance probability from Period I to Period II can be computed by the following equation:

$$\Delta AR_q(p) = AR_q^{II}(p) - AR_q^I(p) \quad (18)$$

For a given non-exceedance probability p , the AR quantile corresponding to the AP quantile $AP_q^I(p)$ is $AR_q^I(p)$ in Period I, while in Period II, the AR quantile corresponding to the AP quantile $AP_q^{II}(p)$ is $AR_q^{II}(p)$. The AR quantile change caused by the change of AP quantile with a given non-exceedance probability p can be computed:

$$\Delta AR_q(p) - AP = f_I(AP_q^{II}(p)) - AR_q^I(p) \quad (19)$$

where f_I indicates the dependence structure between the quantiles of AP and AR in Period I, which is determined by Equation (16).

The effect of other factors excluding the AP can be assessed by the following:

$$\Delta AR_q(p) - NAP = \Delta AR_q(p) - \Delta AR_q(p) - AP \quad (20)$$

Considering the fact that the size of AP and AR series in Period I and Period II may affect the estimation accuracy of AP

and AR quantiles and further influence the reliability of the dependence structure obtained by Equation (16), the Bootstrap method (Hu et al., 2015) is applied to refer the expected estimations of the AP and AR quantile. Then the expected estimations of the AP and AR quantile are used to establish the dependence structure between the quantiles of AP and AR (Equation (16)).

Taking the expected estimation of AR quantile in period I as an example, the bootstrap procedure can be carried out as follows (Hu et al., 2013, 2015). PE3 function contains three parameters: mean value E_x , coefficient of Variation C_v , and coefficient of skewness C_s .

(1) Using Bootstrap method to draw with replacement from the original AR series $X^I = \{x_1, x_2, \dots, x_\tau\}$ to obtain a random sample of size τ (called Bootstrap sample).

(2) Repeating the bootstrap sampling (step (1)) for M times; M groups of bootstrap samples can be obtained, and they are denoted by $B^{*(j)} = (x_1^{*(j)}, x_2^{*(j)}, \dots, x_\tau^{*(j)})$, $j = 1, 2, \dots, M$, and $M = 1000$.

(3) Using the linear-moment method to estimate parameters of each bootstrap sample; gaining M groups of estimations of the three parameters denoted by $\hat{E}_x^{(j)}$, $\hat{C}_v^{(j)}$, $\hat{C}_s^{(j)}$, $j = 1, 2, \dots, M$.

(4) Based on each group of $\hat{E}_x^{(j)}$, $\hat{C}_v^{(j)}$, $\hat{C}_s^{(j)}$, $j = 1, 2, \dots, M$, and for a given non-exceedance probability p , the corresponding estimation of AR quantile $AR_I(p)$ in period I can be acquired. Therefore, M groups of estimation of $AR_I(p)$ can be obtained using M groups of parameters, denoted by $AR_I^{(j)}(p)$, $j = 1, 2, \dots, M$.

(5) Using the series $AR_I^{(j)}(p)$, $j = 1, 2, \dots, M$, the expected estimation of the AR quantile $AR_I(p)$ can be calculated by $E(AR_I(p)) = 1/M \sum_{j=1}^M AR_I^{(j)}(p)$.

3. Results

3.1. Change Point Analysis of AP and AR

The time series of AR and AP are shown in Figure 2. It can be seen that the number of extreme AR and AP after about 1990 is obviously less than that before 1990.

In order to detect the location of the change points, the Pettitt method and the SC method are employed. The testing results show that the AR has the change point with a 5% significant level at 1989 detected by both of the two methods, while for the AP, the change points are 1985 or 1989 (Pettitt) and 1989 (SC) (Figure 3). Finally, the 1989 is selected as the change point for both of the AP and AR. On the basis of the change point of 1989, the whole period 1958 ~ 2007 is divided into two different periods: 1958 ~ 1989 is Period I and 1990 ~ 2007 is Period II.

3.2. Characteristics of AP and AR Before and After the Change Point

To assess the performance of PE3 distribution for fitting the AP and AR series, the Akaike's information criteria (AIC), Bayesian information criterion (BIC) and Kolmogorov-Smirnov test (KS) are used. It can be seen from Table 1 that the PE3

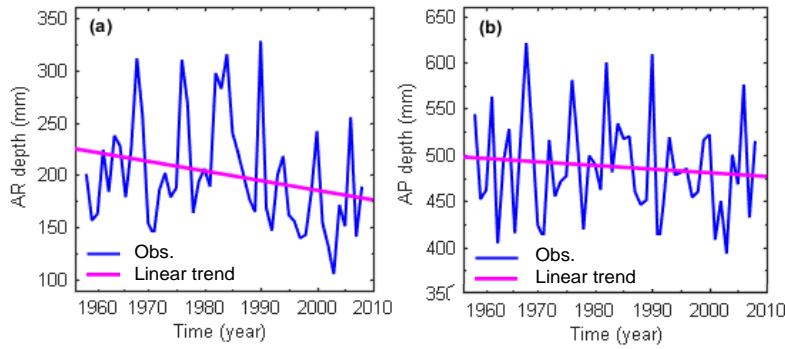


Figure 2. Time series of AR and AP observations. The red line indicates the linear trend of the corresponding series.

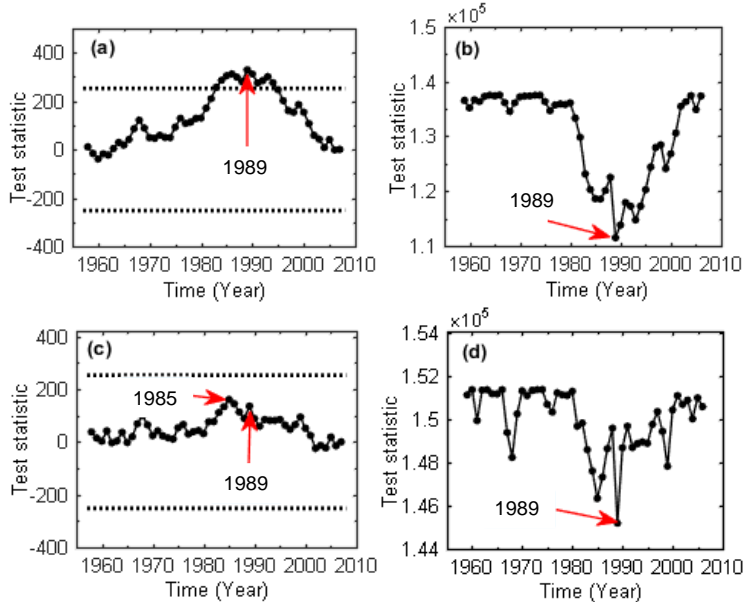


Figure 3. Pettitt((a) and (c)) and Sequential Clustering method ((b) and (d)) for detecting a change point of AR ((a) and (b)) and AP ((c) and (d)). Horizontal line represents the 5% significant level.

Table 1. AIC, BIC, and KS Test Results of PE3

	AP(I)	AP(II)	AR(I)	AR(II)
AIC	354.2	195.6	343.5	185.4
BIC	358.6	198.2	347.9	188.2
KS (<i>p</i> value)	0.987	0.989	0.983	0.978

match the series well and pass the hypothesis test at the significant level of 0.05 that the AP and AR series at Period I and Period II obeys the PE3 distribution.

Figure 4 provides the worm plot (Buuren and Fredriks, 2001; Hu et al., 2017) at 90% confidence level for further assessing the performance of PE3. It can be seen that all point (bias) are located within the 5 and 95% centile curves, and almost all points occur nearby the zero line. This also illustrates that the PE3 match well the AP and AR series and is acceptable for describing the distribution of the AP and AR.

Figure 5 presents the linear relationship between the AP and AR in the two different periods, respectively. It can be seen

that the relationship between the AP and AR in Period II is significantly different from that in Period I. For a given AP event, the corresponding AR in Period II is less than that in Period I.

The Poisson distribution (Siteka and Cellerb, 2015) is used to analyze the probability related to occurrence number of a given extreme AR or AP per year in the two different periods. As can be observed in Figures 6(a) and (b) that the occurrence probability of extreme AR with more than 200 and 150 mm in period II are less than those in period I for the given occurrence numbers of 1, 2, 3, 4 and 5, which means that the occurrence probability of the above extreme AR will become less in the future than that in the past period. Similarly, for the extreme AP with more than 550 and 500 mm (Figures 6(c) and (d)), the corresponding occurrence probability of the above extreme AP will also become less in the future than that in the past period.

3.3. Estimation of AP and AR Quantiles

Figure 7 provides the cumulative distribution function

(CDF) of the AR and AP in the two different periods. It can be observed that the CDFs of AR and AP in Period II are down-shifted compared to those in Period I. This indicates that the quantiles of the AR and AP with given non-exceedance probability in Period II decrease compared to those in Period I.

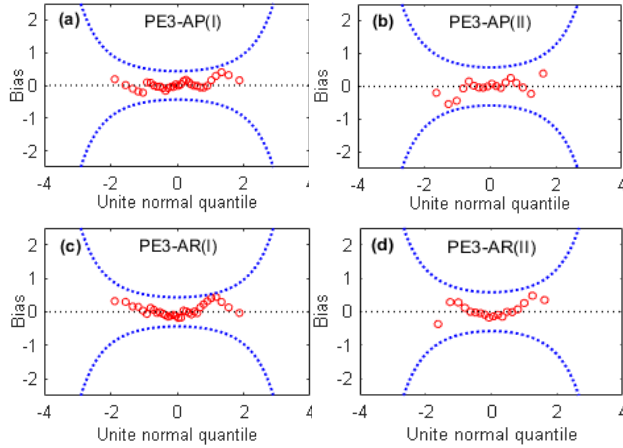


Figure 4. Worm plot for assessing the performance of PE3 function to fit the AP and AR series in Periods I and II. Hollow circles indicate the bias and the two dashed lines mean the 90% confidence interval.

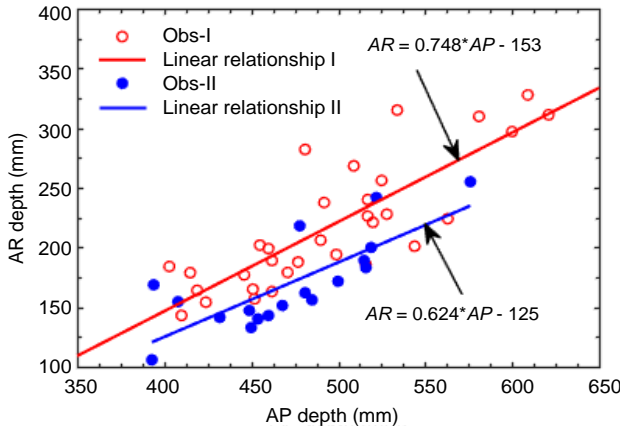


Figure 5. Relationship between AP and AR in two different periods. Obs-I (Obs-II) and Linear relationship I (Linear relationship II) indicate the group of the AP and AR observations and corresponding linear trend in Period I (Period II).

The hydrological frequency analysis (Section 2.3) and Bootstrap method (Section 2.4) are used to refer the expected estimations of the quantiles of AR and AP with given non-exceedance probabilities of 0.8, 0.9, 0.95, 0.98, 0.99, 0.995, 0.998 and 0.999 in the two different periods (Figure 8). It is found that for all given non-exceedance probabilities, the quantiles of AR and AP in period I obviously decrease compared to those in period II. For example, the 0.999-quantile of AR in period I is 472 mm but in period II it is 360 mm, which reduces by 24%; for AP, the 0.999-quantiles are 734 mm in period I and

661 mm in period II, which reduces by 10%.

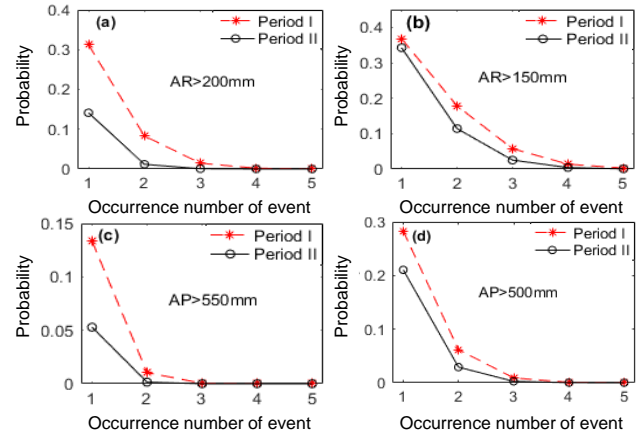


Figure 6. Probability of occurrence number of different events per year in Periods I and II. (a) ~ (b): AR with given thresholds; (c) ~ (d): AP with given thresholds.

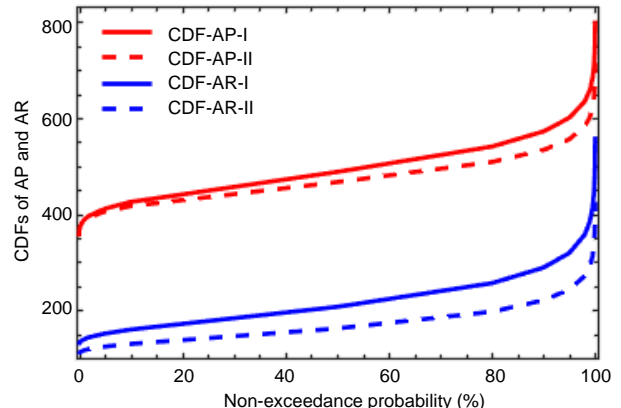


Figure 7. Cumulative distribution function (CDF) of AR and AP in Periods I and II.

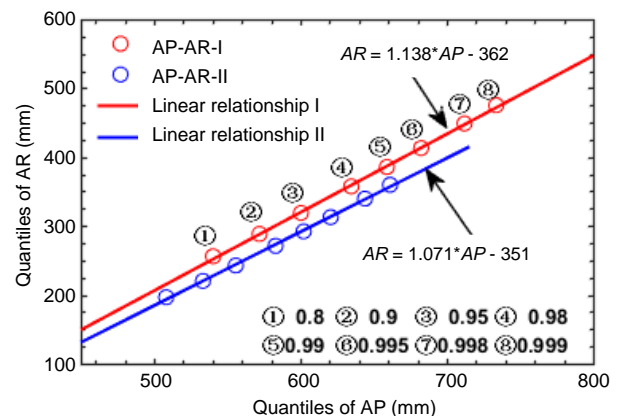


Figure 8. Relationship between the quantiles of AP and AR in Periods I and II. AP-AR-I (AP-AR-II) and Linear relationship I (Linear relationship II) indicate the group of the quantiles of AP and AR and corresponding linear relationship in Period I (Period II).

On the basis of the expected estimations of the above AP and AR quantiles, the linear relationship between the quantiles of AP and AR in the two different periods is established, respectively. As can be seen in Figure 8 that the two AP-AR linear relationship are noticeably different in the two periods. For a given same AP, the corresponding AR in period II is less than that in period I.

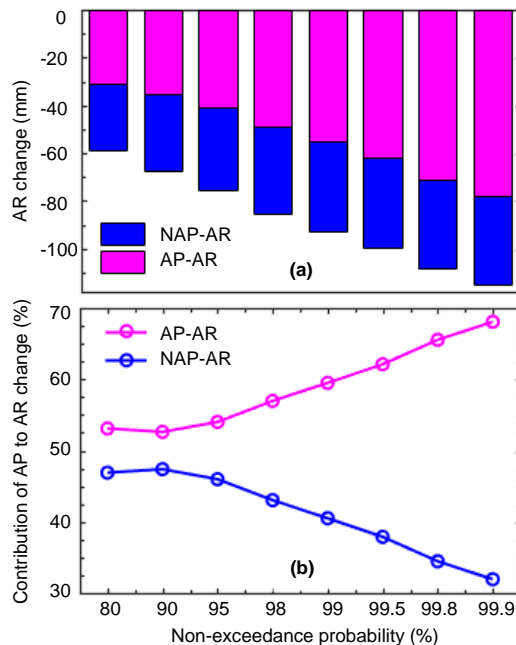


Figure 9. Contribution of AP change to the decrease in AR in terms of the quantiles with given non-exceedance probabilities. AP-AR (NAP-AP) indicates the decrease in AP is caused by AP change (other factors).

3.4. Quantification of AP Change Impact on AR

The dependence structure between AP and the corresponding AR at the level of quantile in period I is estimated by using a linear function to fit AP quantiles and the corresponding AR quantiles (Figure 8). The formula is shown in Equation (21). The coefficient of determination is 0.99, which indicates that the relationship between the quantiles of AP and the corresponding AR is extremely strong:

$$AR'_q(p) = 1.138AP'_q(p) - 362 \quad (21)$$

On the basis of Equation (21), combined with equations (18) ~ (20), the impact of AP change on the AR at the level of quantile is quantified. It can be seen from Figure 9 that the impact of AP change on the AR is dominated for all given non-exceedance probabilities, and with the increase of the probability, its influence gradually become larger. In terms of others factors (all factors excluding precipitation), their impacts on decrease in the AR seems steady for all given probabilities. Taking the 0.999-quantiles as an example, the AR quantile in Period II decrease 115 mm compared to that in Period I, in

which 79 mm is caused by the AP and 36 mm is caused by other factors. For the given eight non-exceedance probabilities from 0.8 to 0.999, the AP change accounts for 53, 53, 54, 57, 60, 62, 66 and 68% of the total decrease of the AR. The contribution of AP change to the decrease in AR becomes larger with the increase of the non-exceedance probability.

4. Conclusions

In this paper, the change characteristics of AP and AR have been analyzed and the impact of AP change on the decrease in AR at the level of quantile has been assessed in the headwater region of Yellow River, China.

A change point at the location of 1989 of the AP and AR is detected by using the Pettitt and Sequential Clustering methods. Before and after the change point, also called Period I and Period II, the relationship between the AP and corresponding AR in Period II (after 1989) is obviously different than that in Period I (before 1989). The Poisson distribution is used to analyze the probability of occurrence number of given extreme AP and AR per year in the two different periods. The occurrence probability of the extreme AR more than 150 mm and extreme AP more than 500 mm become less in Period II than that in Period I.

The CDFs of the AP and AR are obtained and the quantiles of AP and AR with given non-exceedance probabilities of 0.8, 0.9, 0.95, 0.98, 0.99, 0.995, 0.998 and 0.999 are estimated in the two different periods. Overall, the quantiles of AR and AP with given probability in Period II clearly decrease compared to those in Period I. The reduction in the AR is mainly caused by the decrease in the AP. For the given eight non-exceedance probabilities from 0.8 to 0.999, the AP change accounts for 53, 53, 54, 57, 60, 62, 66 and 68% of the total decrease in the AR. The contribution of AP change to the decrease in AR becomes larger with the increase of the non-exceedance probability.

A few previous studies also reported that the precipitation and runoff obviously decrease (Yang et al., 2004; Li et al., 2007; Huang et al., 2009) and the runoff decrease is primarily reflected by the precipitation change as there are no large dams or major irrigation diversions in this study area (Xie et al., 2006; Zhou et al., 2006; Guo et al., 2013). However, different with previous studies, in our study, we aim to analyze the impact of annual precipitation change on annual runoff at the level of quantile.

Excluding AP change effect on AR, the major factors influencing the AR should be temperature, evapotranspiration and permafrost. In past several decades, temperature has risen averagely 0.63 °C in the headwater region of Yellow River. The increase in temperature resulted in the increase of evaporation, which reduced the surface runoff. In addition, the increase of ground temperature leaded to the reduction of the permafrost thickness and the degradation of permafrost; as a result, the infiltration increased and surface runoff decreased. Under the conditions of global climate change, if the temperature in the headwater region of the Yellow River continues to rise, along with the decrease of precipitation, increase of evapotranspira-

tion and degradation of permafrost, the runoff may tend to decrease more, which should be paid more attention on for water resources management and planning.

Acknowledgments. This study was supported by the National Natural Science Foundation of China (41730750, 51709073), the National Key Research projects (2016YFC0402707, 2016YFC0402706), the Natural Science Foundation of Jiangsu Province (BK20170878), and the Fundamental Research Funds for the Central Universities of China (2017B17414). We are also grateful to the editor and all anonymous reviewers for their helpful comments, which helped us to improve the quality of the article.

References

- American Society of Civil Engineers (ASCE, 1996). *Hydrology Handbook*; American Society of Civil Engineers Publications: Reston, VA, USA.
- Bao, Z.X., Zhang, J.Y., Wang, G.Q., Fu, G.B., He, R.M., Yan, X.L., Jin, J.L., Liu, Y.L., and Zhang, A.J. (2012). Attribution for decreasing streamflow of the Haihe River basin, northern China: Climate variability or human activities? *J. Hydrol.*, 460-461, 117-129. <https://doi.org/10.1016/j.jhydrol.2012.06.054>
- Boyer, C., Chaumont, D., Chartier, I., and Roy, A.G. (2010). Impact of climate change on the hydrology of St. Lawrence tributaries. *J. Hydrol.*, 384, 65-83. <https://doi.org/10.1016/j.jhydrol.2010.01.011>
- Buuren, S.V., Fredriks, M. (2001). Worm plot: a simple diagnostic device for modelling growth reference curves. *Stat. Med.*, 20(8), 1259-1277. <https://doi.org/10.1002/sim.746>
- Changjiang Water Resources Commission (CWRC, 1995), *Handbook for Calculating Design Flood of Water Resources and Hydropower Projects*, Nanjing Institute of Hydrology and Water Resources. China Water Power Press, Beijing.
- Ding, J. (1986). Statistical detection for transition point in flood time sequences. *J. Wuhan Univ. Hydraul. Electric Eng.*, 5, 36-41.
- Greenwood, J.A., Landwehr, J.M., Matalas, N.C., and Wallis, J.R. (1979). Probability weighted moments: Definition and relation to parameters of several distributions expressible in inverse form, *Water Resour. Res.*, 15, 1049-1054. <https://doi.org/10.1029/WR015i005p01049>
- Guo, L., Zhang, Y.X., Gao, Y.H., Hao, Z.C., and Cairang, L.S. (2013). The impacts of climate change and land cover/use transition on the hydrology in the upper Yellow River Basin, China. *J. Hydrol.*, 502, 37-52. <https://doi.org/10.1016/j.jhydrol.2013.08.003>
- Hosking, J.R.M. and Wallis, J.R. (1997). *Regional Frequency Analysis*, Cambridge University Press, Cambridge, U.K. <https://doi.org/10.1017/CBO9780511529443>
- Hu, Y.M., Liang, Z.M., Li, B.Q., and Yu, Z.B. (2013). Uncertainty Assessment of Hydrological Frequency Analysis Using Bootstrap Method. *Math. Probl. Eng.*, 2013, 1-7. <https://doi.org/10.1155/2013/175616>
- Hu, Y.M., Liang, Z.M., Liu, Y.W., Zeng X.F., and Wang, D. (2015). Uncertainty assessment of estimation of hydrological design values. *Stochastic Environ. Res. Risk Assess.*, 29(2), 501-511. <https://doi.org/10.1007/s00477-014-0979-z>
- Hu, Y.M., Liang, Z.M., Chen, X., Liu, Y.W., Wang, H.M., Yang, J., Wang, J., and Li, B.Q. (2017). Estimation of design flood using EWT and ENE metrics and uncertainty analysis under non-stationary conditions. *Stoch. Environ. Res. Risk Assess.*, 31(10): 2617-2626. <https://doi.org/10.1007/s00477-017-1404-1>
- Huang, Y., Cai, J.L., Yin, H., and Cai, M.T. (2009). Correlation of precipitation to temperature variation in the Huanghe River (Yellow River) basin during 1957-2006. *J. Hydrol.*, 372, 1-8. <https://doi.org/10.1016/j.jhydrol.2009.03.029>
- Legesse, D., Vallet-Coulomb, C., and Gasse, F. (2003). Hydrological response of a catchment to climate and land use changes in Tropical Africa: Case study South Central Ethiopia. *J. Hydrol.*, 275, 67-85. [https://doi.org/10.1016/S0022-1694\(03\)00019-2](https://doi.org/10.1016/S0022-1694(03)00019-2)
- Li, L.J., Zhang, L., Wang, H., Wang, J., Yang, J.W., Jiang, D.J., Li, J.Y., and Qin, D.Y. (2007). Assessing the impact of climate variability and human activities on streamflow from the Wuding River basin in China. *Hydrol. Process.*, 21, 3485-3491. <https://doi.org/10.1002/hyp.6485>
- Liang, Z.M., Hu, Y.M., Li, B.Q., and Yu, Z.B. (2014). A modified weighted function method for parameter estimation of Pearson type three distribution. *Water Resour. Res.*, 50, 3216-3228. <https://doi.org/10.1002/2013WR013653>
- Ma, H., Yang, D.W., Tan, S.K., Gao, B., and Hu, Q.F. (2010). Impact of climate variability and human activity on streamflow decrease in the Miyun Reservoir catchment. *J. Hydrol.*, 389, 317-24. <https://doi.org/10.1016/j.jhydrol.2010.06.010>
- Miller, J.D., Kim, H., Kjeldsen, T.R., Packman, J., Grebby, S., and Dearden, R. (2014). Assessing the impact of urbanization on storm runoff in a peri-urban catchment using historical change in impervious cover. *J. Hydrol.*, 515, 59-70. <https://doi.org/10.1016/j.jhydrol.2014.04.011>
- Öztürk, M., Copty, N.K., and Saysel, A.K. (2013). Modeling the impact of land use change on the hydrology of a rural watershed. *J. Hydrol.*, 497, 97-109. <https://doi.org/10.1016/j.jhydrol.2013.05.022>
- Pettitt, A. (1979). A nonparametric approach to the change-point problem. *Appl. Stat.*, 28, 126-135. <https://doi.org/10.2307/2346729>
- Pina, J., Tilmant, A., and Anctil, F. (2016). Horizontal approach to assess the impact of climate change on water resources systems. *J. Water Resour. Plann. Manage.*, [https://doi.org/10.1061/\(ASCE\)WR.1943-5452.0000737](https://doi.org/10.1061/(ASCE)WR.1943-5452.0000737).
- Shi, P.J., Yuan, Y., Zheng, J., Wang, J.A., Ge, Y., and Qiu, G.Y. (2007). The effect of land use/cover change on surface runoff in Shenzhen region, China. *Catena*, 69(1), 31-35. <https://doi.org/10.1016/j.catena.2006.04.015>
- Siteka, A. and Cellerb, A.M. (2015). Limitations of Poisson statistics in describing radioactive decay. *Physica Medica*, <https://doi.org/10.1016/j.ejmp.2015.08.015>
- Wang, J., Liang, Z., Wang, D., Liu, T., and Yang, J. (2016). Impact of climate change on hydrologic extremes in the upper basin of the Yellow River Basin of China. *Adv. Meteorol.*, 2016. <https://doi.org/10.1155/2016/1404290>
- Xie, C.W., Ding, Y.J., Han, H.D., and Wang, J. (2006). Analysis on the Runoff Change and its Response to the Climatic Factors at the Source Regions of Yellow River. *J. Arid Land Resour. Environ.*, 20(4), 7-11. (in Chinese)
- Yang, D.W., Li, C., Hu, H., Lei, Z., Yang, S., Kusuda, T., Koike, T., and Musiake, K. (2004). Analysis of water resources variability in the Yellow River of China during the last half century using historical data. *Water Resour. Res.*, 40, <https://doi.org/10.1029/2003WR002763>
- Ye, X.C., Zhang, Q., Liu, J., Li, X.H., and Xu, C.Y. (2013). Distinguishing the relative impacts of climate change and human activities on variation of streamflow in the Poyang Lake catchment, China. *J. Hydrol.*, 494, 83-95. <https://doi.org/10.1016/j.jhydrol.2013.04.036>
- Zhou, D.G. and Huang, R.H. (2006) Exploration of reason of runoff decrease in the source regions of the Yellow River. *Clim. Environ. Res.*, 11(3), 302-309 (in Chinese)